Insulin Signaling in the Yeast *Saccharomyces cerevisiae*. 2. Interaction of Human Insulin with a Putative Binding Protein

Günter Müller,*,‡ Natacha Rouveyre,‡ Claire Upshon,‡ Eva Groβ,§ and Wolfhard Bandlow§

Hoechst Marion Roussel Deutschland GmbH, D-65926 Frankfurt am Main, Germany, and Institut für Genetik und Mikrobiologie der Universität München, D-80638 München, Germany

Received August 20, 1997; Revised Manuscript Received January 8, 1998

ABSTRACT: A putative insulin-binding protein ($K_d = 0.5 \pm 0.2$ μM for human insulin) was partially purified from solubilized plasma membranes of *Saccharomyces cerevisiae* by wheat germ agglutinin and insulin affinity chromatographies. The binding affinities of various mutant insulin analogues correlated well with their capacities to activate glycogen synthase and SNF1 kinase in glucose-induced yeast spheroplasts, the ranking of their relative efficacies in yeast and in isolated rat adipocytes being similar. Using a bifunctional cross-linker and two different experimental protocols, a 53-kDa polypeptide contained in the insulin-binding protein preparation was specifically affinity cross-linked to [^{125}I]monoiodo[B_{26}]insulin. The relative rankings of the insulin analogues with respect to inhibition of cross-linking and binding to the partially purified insulin-binding protein were identical. Incubation of intact yeast spheroplasts with [^{125}I]monoiodo[A_{I4}]insulin led to specific and time-dependent association of the radiolabeled insulin with the cell surface followed by its internalization and degradation. These processes were considerably delayed by low temperature and energy depletion of the spheroplasts, suggesting involvement of the ATP-dependent endosomal apparatus. These data provide evidence for the existence of a low-affinity insulin-binding protein in the plasma membrane of *Saccharomyces cerevisiae*.

In previous studies (*1*; Müller, G., Rouveyre, N., Crecelius, A., and Bandlow, W., preceding paper in this issue), we have demonstrated several metabolic effects of human insulin on *Saccharomyces cerevisiae* cells under two distinct conditions of growth limitation: (i) exhaustion of glucose at late logarithmic phase of cell growth; and (ii) glucose induction of spheroplasts. Insulin was found to activate glycogen synthase, to inhibit glycogen phosphorylase, to increase glycogen synthesis, glucose phosphorylation, and glucose oxidation, and to stimulate SNF1 kinase. In mammalian cells, insulin provokes pleiotropic activation of nonoxidative and oxidative glucose metabolism via a complex intracellular signal transduction pathway (for reviews, see refs *2*−*4*) which is initiated by specific binding of insulin to its receptor protein located at the plasma membrane. Consequently, we looked for a protein in *Saccharomyces cerevisiae* that might bind insulin specifically and be involved in mediating the insulin effects.

EXPERIMENTAL PROCEDURES

Materials. 3-[^{125}I]Monoiodo[B_{26}]insulin (2000 Ci/mmol) and 3-[^{125}I]monoiodo[A_{14}]insulin (1500 Ci/mmol), prepared from human recombinant insulin, were provided by Amersham-Buchler (Braunschweig, Germany). Human recombinant proinsulin and PEG[1] 6000 were obtained from Sigma (Deisenhofen, Germany). Sephacryl S-300HR, Sepharose Cl-4B, and wheat germ agglutinin−agarose were provided by Pharmacia/LKB (Freiburg, Germany). Protease inhibitors and detergents were purchased from Boehringer Mannheim (Mannheim, Germany). Disuccinimidyl suberate was from Pierce (Rockford, IL). All other materials were obtained as described previously (*5*−*7*, see also accompanying papers).

Growth Conditions. Cells from *Saccharomyces cerevisiae* strain X-2180 were grown in 1% yeast extract, 2% bactopeptone, 2% glucose to early logarithmic phase and converted to spheroplasts (5). The spheroplasts were incubated in osmotically stabilized (1.2 M sorbitol) succinate containing medium for 1 h at 37 °C followed by addition of glucose (100 mM final concentration) and hormones as indicated and further incubation for variable periods prior to rapid centrifugation through a cushion of Ficoll/sucrose (for details, see ref *6*).

Partial Purification of the Insulin-Binding Protein. Plasma membranes (15 mg of protein) were prepared from spheroplasts as previously published (6, 8) and finally solubilized in 35 mL of 50 mM Hepes/KOH (pH 7.4), 1% TX-100, 0.1 mg/mL aprotinin, 0.5 mM PMSF, 20 μM leupeptin, 10 μM pepstatin, 25 μM antipain for 30 min at 4 °C. The extract was centrifuged (100000*g*, 1 h, 4 °C). The supernatant (about 30 mL) was applied to a 2-mL wheat germ agglutinin−agarose column (equilibrated with 50 mM Hepes,

* Correspondence should be addressed to this author at Hoechst Marion Roussel Deutschland GmbH, Research Metabolic Diseases, Bldg. H825, D-65926 Frankfurt a.M., Germany. Phone: 0049-69-305-4271. Fax: 0049-69-305-81767. E-mail: Guenter.Mueller@hmrag.com.

‡ Hoechst Marion Roussel Deutschland GmbH.

§ Institut für Genetik und Mikrobiologie der Universität München.

[1] Abbreviations: CCCP, carbonyl cyanide *m*-chlorophenylhydrazone; DNP, 2,4-dinitrophenol; EGF, epidermal growth factor; IGF-1, insulin-like growth factor; PEG, poly(ethylene glycol); SDS−PAGE, sodium dodecyl sulfate−polyacrylamide gel electrophoresis; TCA, trichloroacetic acid.

S0006-2960(97)02072-2 CCC: $15.00
Published on Web 05/27/1998

10 mM $MgCl_2$, 0.1% TX-100) at 4 °C and passed over the column 3 times. Subsequently, the agarose was washed successively with 60 mL of 50 mM Hepes/KOH (pH 7.4), 0.1% TX-100, 0.5 M NaCl, and 200 mL of the same buffer lacking NaCl. Glycoproteins were eluted from the column with 2 mL of 50 mM Hepes (pH 7.4), 300 mM *N*-acetylglucosamine, 0.1% TX-100, 1 mM EDTA, 0.2 mM PMSF, 0.1 mg/mL aprotinin, 10 μM leupeptin, 2 μM pepstatin, 8 mg/mL bacitracin; 8−10 mL of pooled peak binding fractions was applied to a 15-mL insulin−Sepharose column (1.6 × 10 cm, prepared by coupling of insulin to CNBr-activated Sepharose Cl-4B and equilibrated in 50 mM Tris/HCl, pH 7.8, 1 M NaCl, 0.1% TX-100) by recycling the sample 4 times at a flow rate of 5 mL/h. The column was then washed extensively with 50 mM Hepes/NaOH (pH 7.8), 1 M NaCl, 0.6% octyl glucoside (40−60 mL). The insulin-binding protein was eluted from the insulin−Sepharose by passing 20 mL of 50 mM sodium acetate (pH 4.5), 1 M NaCl, 0.6% octyl glucoside, 10% glycerol, 0.2 mM PMSF over the column. One-milliliter fractions of the eluate were collected into tubes containing 100 μL of 1.5 M Hepes/NaOH (pH 8.0). The partially purified insulin-binding protein preparation was desalted and concentrated by ultrafiltration through a concentrator membrane (30 kDa exclusion limit, Centricon-30 miniconcentrator, Amicon No. 4208). Ten 2-mL aliquots were loaded successively into the sample reservoir of the miniconcentrator and centrifuged (3000*g*, 20 min, 4 °C). The concentrated binding protein sample (1−2 mL) in the sample reservoir was supplemented with 2.5 mL of storage buffer (50 mM Hepes/NaOH, pH 7.4, 10% glycerol, 0.6% octyl glucoside, 0.2 mM PMSF, 5 μM leupeptin, 1 μM pepstatin) and centrifuged again. The washing step was repeated once. The concentrated binding protein sample was recovered from the sample reservoir as well as the membrane and used for subsequent studies.

Insulin-Binding Assay. Ten-microliter aliquots of solubilized and partially purified insulin-binding protein in storage buffer (see above) were diluted with 190 μL of assay buffer (50 mM Hepes/KOH, pH 7.4, 150 mM NaCl, 10 mg/mL BSA, 0.2 mM PMSF, 0.5 mM benzamidine) and incubated with 25 μL of [^{125}I]monoiodo[B_{26}]insulin (5×10^6 dpm/mL) in the presence of 25 μL of assay buffer lacking or containing unlabeled insulin (100 μM) for 2 h at 25 °C in 1-mL plastic cups. The assay was terminated by addition of 100 μL of human γ-globulin solution (3 mg/mL) followed by 350 μL of chilled PEG 6000 solution [250 mg/mL in 50 mM Hepes/KOH, pH 7.4, 150 mM NaCl, 0.1% (w/v) TX-100]. After vortexing and incubation for 10 min at 4 °C, the precipitate was centrifuged (9000*g*, 5 min). The supernatant was aspirated and the pellet rinsed once with ice-cold PEG solution (see above but containing 125 mg/mL PEG). The tips of the cups were cut off and measured for radioactivity in a γ-counter (Micromedic Systems, type 2/200).

Cross-Linking of the Insulin-Binding Protein with [^{125}I]-Monoiodo[B_{26}]insulin. Method A. Solubilized and partially purified insulin-binding protein (1−5 μg) in storage buffer (up to 50 μL) was incubated in cross-linking buffer (50 mM Hepes/KOH, pH 7.6, 140 mM NaCl, 5.5 mM KCl, 1.5 mM $CaCl_2$, 1.5 mM $MgSO_4$, 0.1% BSA) with 5.5 nM [^{125}I]-monoiodo[B_{26}]insulin (2 μCi) in the absence or presence of unlabeled human insulin in a total volume of 200 μL for 2 h at 4 °C. After addition of 2 μL of a disuccinimidyl suberate stock solution (5 mM in 100% dimethyl sulfoxide, prepared immediately before use), the incubation was continued for 5 min at 4 °C. The reaction was terminated by adding 50 μL of 1 M Tris/HCl (pH 10.5), 1 mM EDTA and further incubation for 15 min at 4 °C. The sample was precipitated and subjected to SDS−PAGE and autoradiography (Kodak X-Omat AR film) or phosphorimaging (Molecular Dynamics, Storm 840, Krefeld, Germany).

Method B. Fifty-microliter aliquots (4−10 μg) of solubilized and partially purified insulin-binding protein in storage buffer were supplemented with 200 μL of assay buffer and incubated with 100 μM human insulin for 2 h at 25 °C followed by addition of human γ-globulin and precipitation with PEG 6000 as described for the insulin-binding assay (see above). The pellet was then resuspended in 200 μL of 28 mM sodium acetate buffer (pH 4.5) and incubated for 15 min at 4 °C. After addition of 400 μL of PEG 6000 (25% in 0.15 M Tris/acetate, pH 6.8), the mixture was left on ice for 30 min and then centrifuged (15000*g*, 15 min, 4 °C). The pellet was rinsed twice with 1 mL each of PEG 6000 (12.5% in water) and subsequently dissolved in 50 μL of storage buffer for cross-linking with [^{125}]monoiodo-[B_{26}]insulin as described for Method A.

Internalization of [^{125}I]Insulin. Spheroplasts (500 μL, 2×10^6 cells/mL) cultured in medium containing 100 mM succinate, 5 mM $MgCl_2$, 2 mM KH_2PO_4, 5 mM Mes/KOH (pH 6.5), 5 μM thiamin, 1.1 M sorbitol, 0.05% yeast extract for 60 min at 30 °C were incubated with [^{125}I]monoiodo-[A_{14}]insulin in the absence or presence of 100 μM human insulin and in the presence of 100 mM glucose in a shaking water bath. After the periods indicated, halves of the suspensions were supplemented with 1 mL of 20 mM sodium acetate (pH 3.5) plus 1.1 M sorbitol (acid wash) or 20 mM sodium acetate (pH 6.5) plus 1.1 M sorbitol (no acid wash) and then incubated on ice for 15 min. Subsequently, the spheroplasts were separated from the incubation medium by centrifugation through a cushion of Ficoll/sucrose (6). The spheroplast pellets were washed rapidly once each with ice-cold 20 mM sodium acetate (pH 4.5) plus 1.1 M sorbitol in the case of acid wash or sodium acetate (pH 6.5) plus 1.1 M sorbitol in the case of no acid wash, followed by 20 mM Mes/KOH (pH 6.5) plus 1.1 M sorbitol and finally 20 mM Hepes/KOH (pH 7.5) plus 1.1 M sorbitol and then solubilized with 0.5 N NaOH. After neutralization, radioactivity was determined using an LKB1282 γ-counter.

Identification of Insulin Degradation Products Associated with Spheroplasts. Spheroplasts (10 mL, 4×10^6 cells/mL) in medium containing 100 mM succinate, 5 mM $MgCl_2$, 2 mM KH_2PO_4, 20 mM Mes/KOH (pH 6.5), 5 μM thiamin, 1.1 M sorbitol, 0.05% yeast extract were incubated with [^{125}I]-monoiodo[A_{14}]insulin in the presence of 100 mM glucose, then separated from the incubation medium by centrifugation through a cushion of Ficoll/sucrose (6), and finally solubilized in 10 mM Hepes/KOH, 0.1 M KCl, 0.2% TX-100 (at about 0.5 mg/mL protein) for 10 min at 4 °C. After centrifugation (120000*g*, 10 min, 4 °C), the supernatant containing the extract was subjected to HPLC separation (at a flow rate of 1 mL/min) in 0.1 M ammonium buffer (pH 5.5) with an acetonitrile gradient. The precise changes in acetonitrile concentration required to effect the separation of degradation intermediates were as follows: (1) 0−5 min

at 0%, (2) 5−20 min gradient rising to 8.45%, (3) instantaneous rise to 28.5%, (4) 20−40 min gradient rising to 32.5%. Detection of ^{125}I was achieved by an on-line counter attached to a reverse phase HPLC Hypersil-BDS, 5 μM, C-18 column, 250 × 4.6 mm, fitted with an additional 10-mm guard cartridge of the same material (Shandon, Cheshire, U.K.). For TCA precipitation of insulin, 250-μL portions of the extract were added to 500 μL of ice-cold 20% TCA and incubated on ice for 10 min prior to centrifugation (15000*g*, 10 min, 4 °C). The pellet (washed once with 5% ice-cold TCA and solubilized with 0.5 N NaOH) and the supernatant were then counted for radioactivity using an LKB 1282 γ-counter.

Miscellaneous. Published procedures were used for preparation of spheroplasts by Zymolyase digestion (5), measurement of glycogen synthase and SNF1 kinase activities (Müller, G., Rouvevyre, N., Crecelius, A., and Bandlow, W., preceding paper in this issue, SDS−PAGE and fluorography (9), protein determination (10), and protein precipitation (11). All data analysis was performed using SigmaPlot for Windows 4.0 statistical software.

RESULTS

Human Insulin Interacts Specifically with Plasma Membranes of Yeast. The finding that human insulin apparently specifically modulates the activity of a number of distinct enzymes in *Saccharomyces cerevisiae* engaged in the control of glucose and glycogen metabolism (e.g., glycogen synthase, SNF1 kinase; see ref *1*; Müller, G., Rouveyre, R., Crecelius, A., and Bandlow, W., preceding paper in this issue) raised the question about the nature of the underlying signaling mechanism. In the present study, we looked for a specific insulin-binding protein in the plasma membrane of yeast spheroplasts that might be functionally analogous to the mammalian insulin receptor (for reviews, see refs *12*, *13*). We applied the purification method commonly used to isolate the insulin receptor from rat liver (14). Solubilized plasma membrane proteins were prepared from glucose-induced spheroplasts (60 min after addition of glucose) and adsorbed to wheat germ agglutinin−agarose, and the affinity-bound material was eluted with an *N*-acetylglucosamine-containing buffer (see Experimental Procedures). The eluate was passed through an insulin−Sepharose column. The protein fraction eluted at acid pH was neutralized, concentrated, and assayed for binding of human [^{125}I]monoiodo[B_{26}]insulin. Binding was performed in the absence and presence of 100 μM unlabeled human insulin and terminated by precipitation of the proteins with PEG and rapid filtration. Figure 1A shows total (squares) and nonspecific (i.e., presence of excess of unlabeled insulin; open circles) binding of [^{125}I]insulin over a wide range of concentrations (for better resolution, the initial insulin concentrations are depicted in an inset using a larger scale). The binding assay was performed routinely with an amount of protein at the upper limit of linearity between the amount of insulin bound and insulin-binding protein used (data not shown). Under these conditions, nonspecific binding accounted for up to 25% of the total insulin bound at 1 μmol of insulin. The resulting specific insulin binding (Figure 1A, filled circles) displayed a typical saturation curve. According to Scatchard plot analysis (Figure 1B, filled circles), these data fitted best with two binding sites with K_d values of 350−500 nM and 20−50

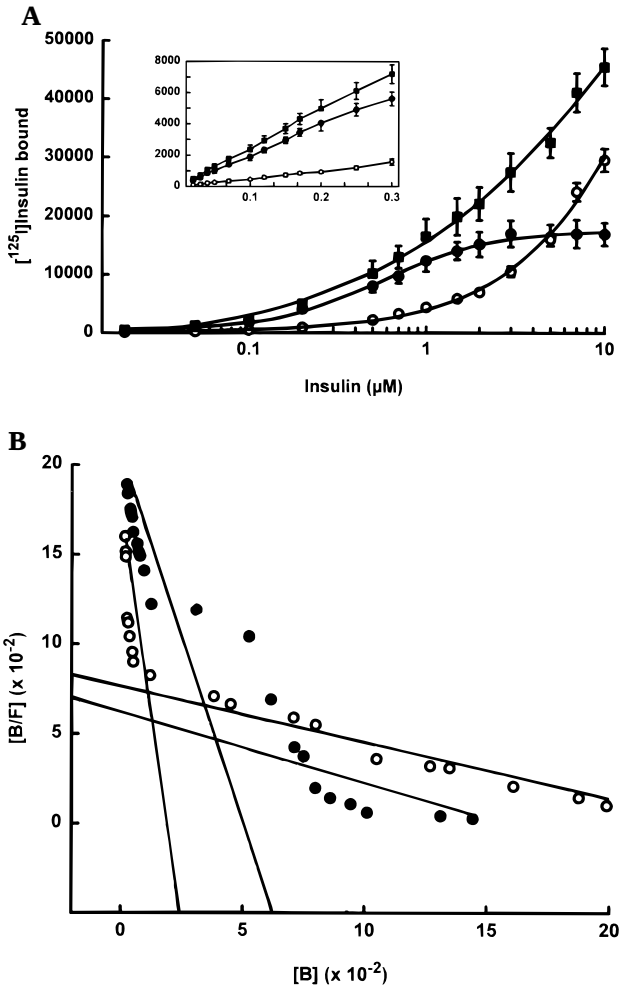

FIGURE 1: Binding of human insulin to yeast plasma membranes. Panel A: Increasing amounts of human [^{125}I]monoiodo[B_{26}] were incubated with 2 μg of insulin-binding protein partially purified from glucose-induced spheroplasts (Experimental Procedures). Incubation was performed in the absence (squares) or presence of 100 μM human unlabeled insulin (open circles) and then terminated by precipitation with PEG 6000. The precipitate was counted for radioactivity. Specific binding of [^{125}I]monoiodo[B_{26}]insulin (filled circles) was calculated as the difference between total binding (squares) and unspecific binding (open circles). The points represent means ± SEM of at least 6 different binding protein preparations with binding assays performed in triplicate, each. The inset shows the binding at low insulin concentrations in detail. Panel B: Specific binding of [^{125}I]monoiodo[B_{26}]insulin using binding protein from glucose-induced spheroplasts (filled circles) or from spheroplasts incubated in osmotically stabilized succinate medium (open circles). The binding data were fitted as Scatchard plots using the program LIGAND (32) for nonlinear regression curve fitting of complex (two-site binding and two-site competition model) radioligand−binding site interactions. [B], bound insulin; [F], free insulin

μM and B_{max} values of 0.5−1.5 and 10−20 pmol/μg of protein, respectively (contained in the insulin-binding protein preparation), corresponding to about 70 and 1500 pmol/mg of plasma membrane protein. Binding affinity as well as the number of binding sites was similar for the insulin-binding proteins prepared from spheroplasts which had been incubated with glucose (filled circles) or with succinate (open circles). The binding affinity of the more potent binding site is in reasonable agreement with the insulin concentrations required for stimulating glucose metabolism (not shown here, but see ref *1*; Müller, G., Rouveyre, N., Crecelius, A., and Bandlow, W., preceding paper) and glycogen synthase in

Table 1: Correlation of the Affinity to the Insulin-Binding Protein and Biological Effects of Human Insulin and Insulin Analogues[a]

	glycogen synthase	SNF1 kinase	binding
human insulin	100 (0.3)	100 (0.6)	100
analogue I	45 ± 8	69 ± 9	81 ± 7
analogue II	25 ± 6	38 ± 11	49 ± 5
analogue III	10 ± 3	16 ± 8	6 ± 2
analogue IV	0	3 ± 1	0
IGFI	30 ± 9	44 ± 15	33 ± 8
EGF	5 ± 2	8 ± 3	2 ± 2

[a] Glycogen synthase and SNF1 kinase were measured in glucose-induced (100 mM) spheroplasts incubated in the absence or presence of insulin, insulin analogues I, II, III, and IV, IGF1, and EGF at 1 μM final concentration each for 60 min. For SNF1 kinase activity, the amount of (auto)phosphorylated SNF1 protein was measured by immunoprecipitation using a specific anti-SNF1 antibody. The difference in the glycogen synthase and SNF1 kinase activities measured between hormone-treated and basal spheroplasts is given as a percentage of the maximal insulin effect (set at 100%). Binding was assayed as displacement of [^{125}I]monoiodo[B_{26}]insulin by 10 μM unlabeled competing hormone (see Figure 2). The amount of radiolabeled insulin displaced by human insulin (difference between total and unspecifically associated insulin) was set at 100%. Each value represents the mean ± SEM of at least three different binding protein preparations with assays performed in triplicate. The EC_{50} values (micromolar) for human insulin are given in parentheses. For structures of the insulin analogues, see the legend to Figure 2.

yeast spheroplasts (see Table 1; EC_{50} about 300 nM, maximal activity at 1 μM), but is 2 orders of magnitude lower than that of typical mammalian insulin receptors (K_d values in the nanomolar range). The number of these "low"-affinity binding sites in yeast spheroplasts ($3-9 \times 10^3$ per spheroplast), however, lies in the range of the number of insulin receptors detected in vertebrate tissues which varies from as few as 40 receptors on circulating erythrocytes to more than 2×10^5 receptors in adipocytes and hepatocytes.

To substantiate the specificity of binding of human insulin, competitive binding assays were performed, and displacement of [^{125}I]monoiodo[B_{26}]insulin by unlabeled human insulin and various insulin analogues was measured (Figure 2). The mutant insulins with defined amino acid substitutions (see legend to Figure 2) have been demonstrated to exhibit slightly lower (analogue I), considerably lower (analogues II and III), or no (analogue IV) biological activity in both isolated rat adipocytes and yeast spheroplasts (Table 1). The displacement curves (Figure 2) were of typical sigmoidal shape with the unspecific component at about 20% of total binding. As expected, displacement was most efficient with human insulin (filled circles; $IC_{50} = 0.5$ μM; the IC_{50} values have been corrected for unspecific binding) followed by the analogues I (open circles; $IC_{50} = 2$ μM), II (triangles; $IC_{50} = 10$ μM), and III (filled squares; $IC_{50} = 50$ μM), whereas analogue IV (open squares) did not compete significantly up to 2.5 mM. Taken together, the data on saturable and displaceable binding of human insulin argue in favor of the presence of a specific insulin-binding protein in yeast plasma membranes. Binding experiments with total cellular membranes or isolated plasma membranes did not yield reliable results irrespective of whether used in the intact or solubilized state (data not shown). The high unspecific binding combined with the relatively low number of binding sites present in the yeast plasma membrane obviously necessitates partial purification and enrichment of the putative yeast insulin-binding protein in order to allow detection by assaying binding.

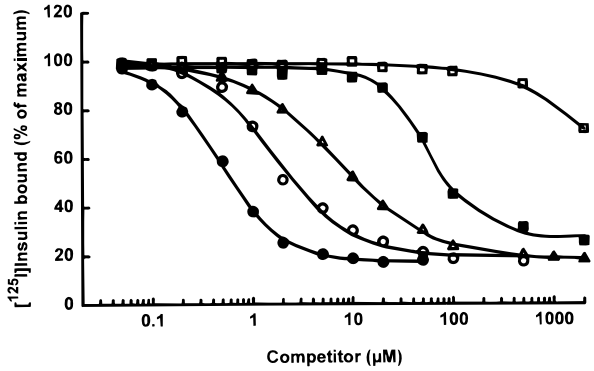

FIGURE 2: Competition of binding of human insulin by insulin analogues. Two micrograms of partially purified insulin-binding protein from glucose-induced yeast spheroplasts was incubated with [^{125}I]monoiodo[B_{26}]insulin in the presence of increasing concentrations of unlabeled human insulin (filled circles) or insulin analogues I (open circles), II (triangles), III (filled squares), or IV (open squares). Further processing was performed as described for Figure 1A. Total binding of human [^{125}I]monoiodo[B_{26}]insulin in the absence of competing insulin analogue was set at 100%. The points represent the means of three different binding protein preparations with binding assays performed in quadruplicate. EC_{50} values were calculated by fitting the data to sigmoidal concentration−response curves. Best of fit was estimated from R^2 and sum-of-squares values. The insulin analogues have the following structures: analogue I, Lys(B3)-Glu(B29); analogue II, Gly(A21)-diLys(B31); analogue III, Gly(A21)-His(B1)-His(B3)-diArg(B31); analogue IV, Met(A3)-Gly(A21)-His(B31)-Ala(B32)-Ala(B33)-Arg(B34).

Human Insulin Can Be Cross-Linked to a Plasma Membrane Protein from Yeast. The putative insulin-binding protein was identified by means of chemical cross-linking with the noncleavable, homobifunctional cross-linking agent disuccinimidyl suberate. Since cross-linking of insulin to the mammalian insulin receptor by disuccinimidyl suberate predominantly occurs via the B-chain of insulin (15, 16), the experiments were performed using [^{125}I]monoiodo[B_{26}]-insulin to enable detection by reducing SDS−PAGE analysis. For this, detergent-solubilized and partially purified binding protein preparation (for Coomassie staining pattern, see lane 1 of Figure 3A) was incubated with [^{125}I]monoiodo[B_{26}]-insulin in the absence or presence of excess unlabeled human insulin. Cross-linking was initiated by addition of disuccinimidyl suberate and terminated by supplementation of excess of Tris. Total precipitated cross-linked products were separated by reducing SDS−PAGE. The autoradiography of the gel (Figure 3A) identified several radiolabeled polypeptides with molecular masses ranging from 85 to 31 kDa (lane 4). The labeling of a 58-kDa cross-linked product (arrowhead) was completely abolished in the presence of 5.5 μM unlabeled insulin during the binding step (lane 3), whereas radiolabeling of the other products (85, 70, 66, 54, 51, 31 kDa) was moderately reduced, only. The latter polypeptides remained detectable even in the presence of 55 μM unlabeled insulin (lane 2), and, most likely, they were unspecifically associated with [^{125}I]monoiodo[B_{26}]insulin. A protein of similar size as the 70-kDa cross-linked product (lane 4, arrowhead) represented a major component of the protein preparation used (lane 1). However, considering the apparent molecular mass of the cross-linked insulin B-chain, these polypeptides were not identical. However, it cannot

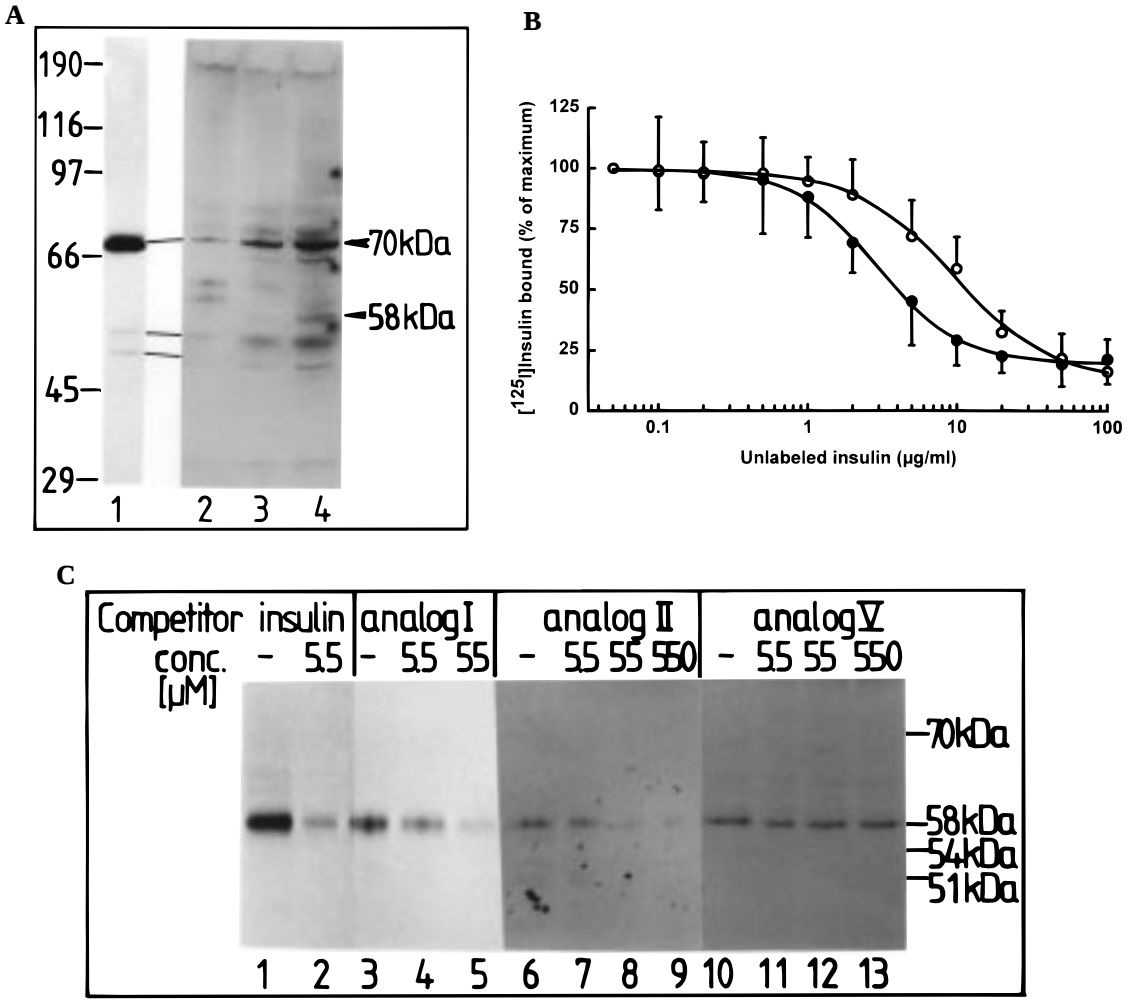

FIGURE 3: Cross-linking of the insulin-binding protein with [^{125}I]monoiodo[B_{26}]insulin. Panels A and B: 5 μg of partially purified insulin-binding protein from glucose-induced spheroplasts was incubated with [^{125}I]monoiodo[B_{26}]insulin in the presence of 55 μM unlabeled human insulin (lane 2) or 5.5 μM human insulin (lane 3) or various concentrations of human insulin as indicated (panel B, filled circles) or without further additions (panel A, lane 4). After cross-linking using disuccinimidyl suberate, the products were analyzed by reducing SDS−PAGE and autoradiography (panel A) or phosphorimaging (panel B) (see Experimental Procedures). Lane 1 of panel A shows a Coomassie blue stain of 10 μg of insulin-binding protein preparation. The experiment shown was repeated several times with similar results. The arrowheads point to the two major cross-linked proteins with apparent molecular masses of 70 and 58 kDa (corresponding to about 65 and 53 kDa, respectively, when the mass of the insulin B-chain is subtracted). Panel B: The amount of cross-linked radiolabeled insulin determined for the 58-kDa band by phosphorimaging in the absence of competitor was set at 100% (open circles). Total binding of [^{125}I]monoiodo[B_{26}]insulin to the insulin-binding protein in the presence of increasing concentrations of unlabeled human insulin was determined as described in the legend to Figure 2 and is given as percent of total binding in the absence of competitor (set at 100%; filled circles). The points represent means ± SD of at least four independent cross-linking or binding experiments, each. Panel C: 8 μg of partially purified insulin-binding protein from glucose-induced spheroplasts was incubated with 100 μM human insulin and subsequently precipitated with PEG 6000. The pellet was subjected to acid wash (as described under Experimental Procedures) and precipitated again. The dissolved insulin-binding protein was incubated with [^{125}I]monoiodo[B_{26}]insulin in the absence or presence of human insulin or various insulin analogues at the concentrations indicated. After cross-linking using disuccinimidyl suberate, the products were analyzed by reducing SDS−PAGE and autoradiography. The relative positions of the cross-link products obtained with method A (see panel A) and run in parallel on the same gel are indicated on the right margin. The experiment was repeated twice with comparable results. Insulin analogue V = human proinsulin; for the structure of the other analogues, see the legend to Figure 2.

be excluded that bovine serum albumin (66 kDa; added to the reaction mixture but absent from the sample of lane 1) was cross-linked to [^{125}I]monoiodo[B_{26}]insulin in a nonsaturatable fashion. Considering the size of the cross-linked insulin B-chain, the insulin-binding protein specifically labeled as a 58-kDa species has an apparent molecular mass of 53−55 kDa. No major polypeptide of comparable size was detected in the protein preparation using Coomassie staining as a criterion (lane 1). Nonreducing conditions of the SDS−PAGE did not affect the relative mobility of the 58-kDa cross-linked product (data not shown), indicating that it is not disulfide-linked to another polypeptide under native conditions. Control experiments demonstrated the strict dependence of the labeling pattern on the inclusion of disuccinimidyl suberate following the binding reaction and on the use of a native protein preparation (in contrast to a preparation denatured by heating at 95 °C for 5 min or treatment at pH 4.2 or incubation with 2% SDS before or after incubation with insulin prior to cross-linking; data not shown). Affinity cross-linking with total membranes or isolated plasma membranes from yeast spheroplasts in the absence or presence of detergent resulted in unspecific radiolabeling of numerous proteins (17−96 kDa; no reduction of labeling even at 500 μM unlabeled insulin; data not

shown) but failed to identify a specific insulin-binding protein, e.g., the 53-kDa polypeptide (possibly masked by "background labeling"), presumably for the same reasons mentioned above for detection of specific binding. The specificity of affinity cross-linking of the 53-kDa polypeptide to [^{125}I]monoiodo[B_{26}]insulin by disuccinimidyl suberate was examined by quantitatively comparing the efficiency of its competition with that of displacement of binding of [^{125}I]-monoiodo[B_{26}]insulin to the partially purified insulin-binding protein preparation by increasing concentrations of human insulin (present during the cross-linking and binding reactions, respectively; Figure 3B). Affinity cross-linking (open circles) and binding (filled circles) of this radiolabeled ligand were diminished by excess human insulin within the same concentration range with IC_{50} values of 2 and 0.7 μM, respectively. Unspecific cross-linking and binding accounted for about 25% in both cases.

We tried to reduce the apparently unspecific cross-linking of some polypeptides contained in the insulin-binding protein preparation (e.g., 70, 54 kDa; see Figure 3A) by pretreatment with excess of human insulin and subsequent removal of the insulin molecules bound specifically, only, leaving unspecific binding sites covered with insulin. It is well-known that the interaction between mammalian insulin and insulin receptor can be weakened in a dramatic but reversible manner by lowering the pH (17, 18). Consequently, we subjected the precipitates of solubilized and partially purified insulin-binding protein preparation which had been incubated with 100 μM human insulin before precipitation to an acid wash (at pH 3.5) for a short period at 4 °C. After adjustment of the pH and precipitation, cross-linking with [^{125}I]monoiodo-[B_{26}]insulin using disuccinimidyl suberate was performed. The autoradiogram of the SDS−PAGE analysis demonstrates that this alternate method led to cross-linking of a 58-kDa protein, exclusively (Figure 3C, lane 1), which was almost completely blocked by excess of unlabeled human insulin (lane 2). Presumably, only insulin specifically bound to this protein during the preincubation period was released during the acid wash whereas the unspecific interactions between insulin and the other polypeptides (e.g., 70, 54, 51 kDa) resisted treatment with low pH. The insulin molecules remaining associated may thereby block subsequent (unspecific) cross-linking. The specificity of this cross-linking procedure was strengthened by the finding that different insulin analogues (for structures, see legend to Figure 2) compete for the cross-linking of the 58-kDa protein in a different manner according to their relative affinities to the partially purified insulin-binding protein as determined by competition of equilibrium binding (see Figure 2) as well as according to their relative efficacies in rat adipocytes. Analogue I (lanes 3−5) was less efficient than human insulin in inhibiting crosslinking but more potent compared to analogue II (lanes 6−9), whereas analogue V (lanes 10−13) had no effect at all on the amount of labeled 58-kDa protein, even at 550 μM final concentration. Taken together, these observations provide strong evidence that the 53-kDa polypeptide is the specific insulin-binding protein in yeast plasma membranes corresponding to the "low"-affinity binding site as revealed by Scatchard plot analysis (see Figure 1B).

Internalization and Degradation of Radiolabeled Insulin by Spheroplasts. As a first hint for a physiological role of the insulin-binding protein in yeast, we studied whether intact spheroplasts are able to specifically bind, internalize, and degrade insulin upon exposure to this ligand in the incubation medium as has been known for insulin-sensitive mammalian cells for decades (*19*−*22*). For discrimination between cell surface-bound and internalized insulin, we took advantage of the observed acid sensitivity of the interaction between human insulin and the yeast insulin-binding protein (see above). For characterization of the putative uptake mechanism, we used the uncouplers of mitochondrial respiration, DNP and CCCP, as well as lowering of the temperature during incubation of the spheroplasts with insulin. It has been amply documented that the internalization of insulin in mammalian cells, which involves the endosomal system, is an energy-dependent and temperature-sensitive process (*23*, *24*; for a review, see ref *25*).

Incubation of spheroplasts derived from glucose-grown yeast cells with [^{125}]monoiodo[A_{14}]insulin at either 30 °C (circles) or 4 °C (triangles) resulted in a steady-state level of specific total cell-associated radioactivity within 45 and 90 min, respectively (Figure 4A). The kinetics for acid-resistant radioactivity showed that the slow rate of reaching steady state was due entirely to the kinetics of intracellular appearance of the label, i.e., internalization, as manifested in the specific acid-resistant radioactivity at 30 °C (squares) and 4 °C (diamonds). Maximal specific surface binding of ^{125}I-labeled insulin, calculated as the difference between total and acid-resistant radioactivity (Figure 4B), was reached at 30−40 min of incubation at 30 °C (circles) and 4 °C (squares) and then remained unchanged throughout the experimental period. The uncoupling agents, DNP and CCCP, increased the total cell-associated radioactivity, which reached a maximum after 60 min of incubation at 30 °C (data not shown), whereas the acid-resistant radioactivity (Figure 4A) was reduced dramatically at the same time in the presence of DNP (houses) or CCCP (inverted triangles) compared to incubation at 30 °C in the absence of agent (squares). The calculated surface-bound ^{125}I-labeled insulin (Figure 4B) in the presence of DNP (triangles) or CCCP (diamonds) reached a level about twice as high as that obtained in the absence of uncouplers (squares). The acid wash procedure permits determination of both surface-bound and internalized ^{125}I-labeled insulin, the latter including the pool of intact and degraded ^{125}I-labeled insulin no longer associated with the putative insulin-binding protein. Consequently, the surface-associated ^{125}I-labeled insulin is the best measure for the effect of temperature and uncoupling on internalization of insulin and the insulin-binding protein putatively involved. The saturability of the binding as well as the internalization of ^{125}I-labeled insulin to spheroplasts was documented as competition of cell surface-associated and internalized radioactivity by increasing concentrations of human insulin (Table 3). The IC_{50} values which were similar for both processes also closely resembled that for binding of ^{125}I-labeled insulin to the partially purified insulin-binding protein (see Figure 2). Taken together, these experiments suggest that human insulin associates with the surface of yeast spheroplasts in a specific, i.e., saturatable, and time-dependent fashion and is subsequently internalized in a time-dependent and energy-consuming manner, both processes presumably being mediated by the 53-kDa insulin-binding protein.

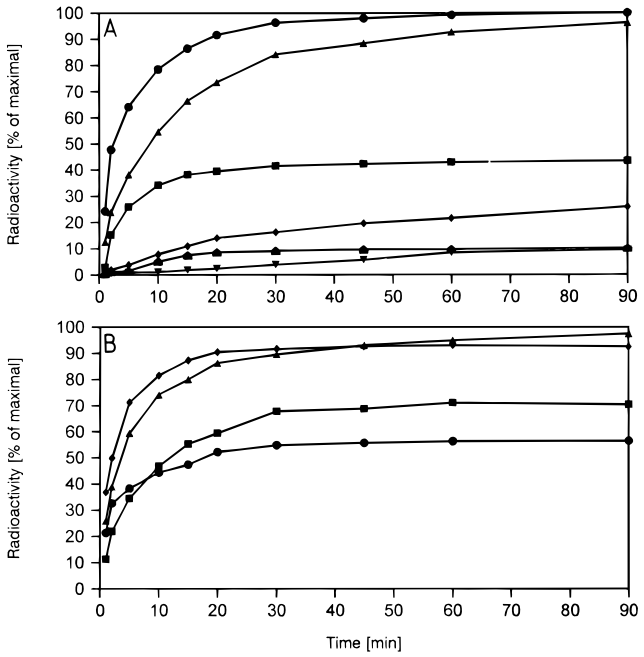

FIGURE 4: Kinetics of the internalization of [^{125}I]monoiodo[A_{14}]-insulin in spheroplasts. After glucose induction of the spheroplasts (as described under Experimental Procedures), DNP (in ethanol, 1 mM final concentration) or CCCP (in ethanol, 200 μM final concentration) or an equivalent volume of ethanol (control) was added, and the incubation was continued for 10 min at 30 °C. Thereafter, the spheroplasts were incubated with 10 μCi of [^{125}I]-monoiodo[A_{14}]insulin in the absence or presence of 100 μM insulin for various periods at 30 °C (control and DNP- and CCCP-treated cells) or 4 °C (control cells). After adjustment of the incubation medium to pH 6.5 (no acid wash) or 3.5 (acid wash) by addition of 20 mM sodium acetate, the spheroplasts were centrifuged through a cushion of Ficoll/sucrose. Panel A: Total (no acid wash; circles, triangles) and acid-resistant (acid wash; squares, diamonds, houses, inverted triangles) specifically cell-associated radioactivity was determined as the difference between radiolabeled insulin bound in the absence and presence of 100 μM insulin. Data are shown for spheroplasts incubated at 4 °C (triangles, diamonds) or 30 °C in the absence (circles, squares) or presence of CCCP (houses) or DNP (inverted triangles). Panel B: The amount of radioactivity specifically associated with the cell surface of spheroplasts, which have been pretreated with DNP (diamonds), CCCP (triangles), or ethanol alone (squares) at 30 °C or ethanol alone (circles) at 4 °C, was calculated as the difference between total (no acid wash) and intracellular (acid wash) radioactivity (see panel A). Each value represents the mean of four separate incubations using spheroplasts from two independent preparations. Each experiment is normalized by setting the total specific binding obtained with unpoisioned spheroplasts after 90 min at 30 °C (panel A) at 100%. Actual dpm for this value varied from 8000 to 11 000 with 1500 to 4000 nonspecific. The SD values were in the range of 11−18% of the means.

Next we analyzed the intactness of the [^{125}]monoiodo[A_{14}]-insulin associated with intact spheroplasts (cell surface-bound plus internalized) during increasing periods of incubation at 30 °C under the conditions of the equilibrium binding and cross-linking assays (Figure 5). HPLC separation of the total cell-associated radioactivity revealed a significant reduction of the amount of intact insulin (migrating as peak 3) from 15 min (100%; panel A) to 30 min (73.6%; panel B) and 60 min (24.3%; panel C) of incubation. The major insulin degradation product, the amount of which increased in a time-dependent fashion (peak 2), was identified as deshexapeptide insulin (having lost the six carboxy-terminal amino acids of the B chain) which has often been observed as a common

Table 2: Integrity Determination of ^{125}I-[A_{14}]Insulin Associated with Yeast Spheroplasts by TCA Precipitation[a]

incubation period (min)	incubation temperature			
	30 °C		4 °C	
	dpm	% of total	dpm	% of total
5	44459 ± 6722	100	30561 ± 5822	100
15	39124 ± 4520	88	32983 ± 6132	108
30	25512 ± 4788	57	28450 ± 4359	93
60	12107 ± 3027	27	26983 ± 5104	88
120	3041 ± 1056	7	22587 ± 3977	74
480	1019 ± 443	2	15138 ± 2144	49

[a] The experiment was performed as described in the legend to Figure 5 with the incubation periods and at the temperatures indicated, but performing TCA precipitation of total extracts from spheroplasts as described under Experimental Procedures. The values represent the mean ± SD of three independent incubations using spheroplasts from two different preparations.

Table 3: Saturability of the Internalization of [^{125}I]Monoiodo[A_{14}]insulin[a]

human insulin (μM)	% cell surface-bound insulin	% internalized insulin
−	100	100
0.1	95 ± 6	104 ± 8
0.3	78 ± 12	89 ± 10
1	61 ± 15	70 ± 17
3	35 ± 10	45 ± 20
10	19 ± 5	27 ± 13
100	14 ± 5	22 ± 9

[a] Glucose-induced spheroplasts were incubated with 10 μCi of [^{125}I]monoiodo[A_{14}]insulin in the absence or presence of increasing concentrations of human insulin for 20 min at 30 °C. After adjustment of the incubation medium to pH 6.5 (no acid wash) or 3.5 (acid wash) by addition of 20 mM sodium acetate, the spheroplasts were centrifuged through a cushion of Ficoll/sucrose. The amount of cell surface-bound radiolabeled insulin was calculated as the difference between the total (no acid wash) and acid-resistant cell-associated radioactivity which represents the amount of internalized radiolabeled insulin. Each value represents the mean ± SD of three separate incubations using spheroplasts from two independent preparations. Each experiment is normalized by setting the insulin bound to the cell surface or internalized at 100% each.

cleavage product of (human) insulin in mammalian systems. The data were in good agreement with the time course for insulin degradation at 30 °C using the less stringent criterion of TCA precipitability (Table 2). At 4 °C, the kinetics were considerably delayed, consistent with the lower rate of internalization defined as acid-resistant cell-associated radioactivity (see Figure 4A). Interestingly, after energy depletion of the spheroplasts by uncoupling with CCCP prior to incubation with ^{125}I-labeled insulin, a significantly higher amount of intact insulin was found to be cell-associated (144.3%; Figure 5, panel D) than recovered with respiring cells (set at 100% in panel A). The markedly diminished degradation of ^{125}I-labeled insulin correlated positively with its impaired internalization (see Figure 4A) and elevated cell surface binding (see Figure 4B) caused by either energy depletion or low temperature. This suggests that human insulin is proteolytically cleaved inside the spheroplasts upon delivery into the endosomal system.

The specificity of the binding of [^{125}]monoiodo[A_{14}]insulin to intact spheroplasts was assessed by studying its competition with excess of unlabeled insulin analogues or growth factors (Figure 6). The assay was performed at 4 °C

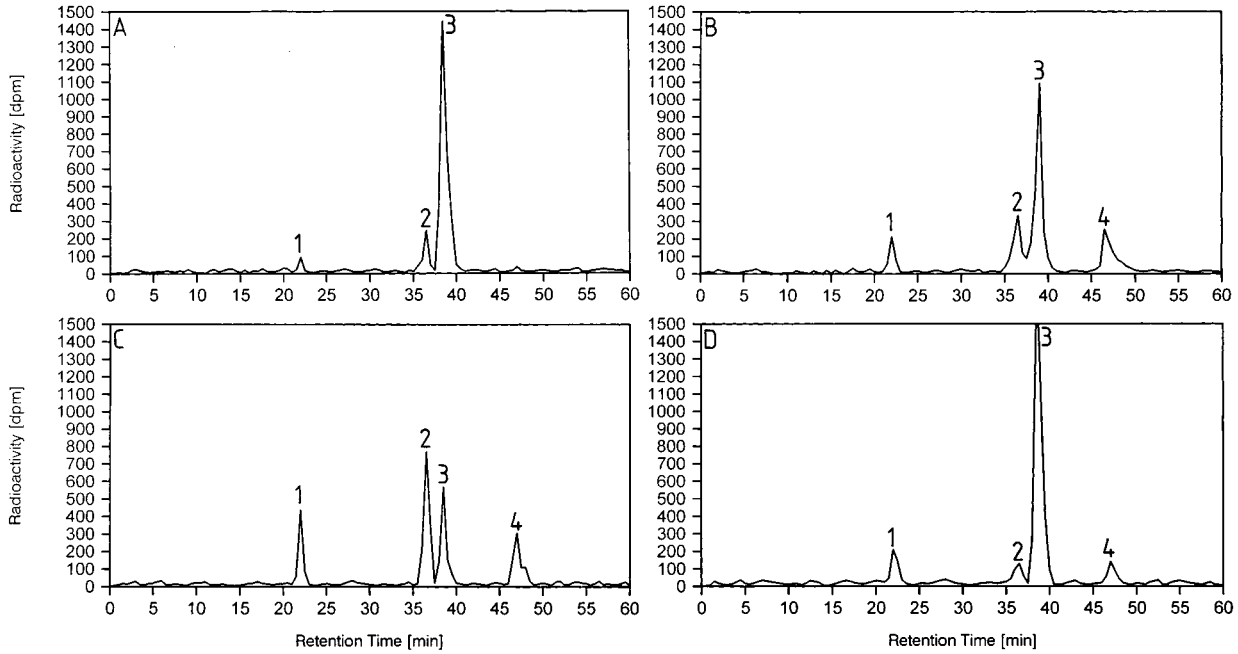

FIGURE 5: Integrity determination of [^{125}I]monoiodo[A_{14}]insulin associated with spheroplasts by HPLC analysis. Untreated (panels A−C) or pretreated (10 min, 200 μM CCCP, 30 °C; panel D) spheroplasts were incubated with 10 μCi of [^{125}I]monoiodo[A_{14}]insulin for 15 min (panel A), 30 min (panel B), or 60 min (panels C, D) as described under Experimental Procedures. The spheroplasts were separated from the incubation medium by centrifugation, extracted with 0.2% TX-100, and subjected to HPLC analysis. The peak materials have been identified as follows: peak 1, iodine; peak 2, deshexapeptide; peak 3 intact insulin; peak 4, unknown. The figure represents a typical experiment repeated 6 times with similar results using spheroplasts from two different preparations by performing three separate incubations, each.

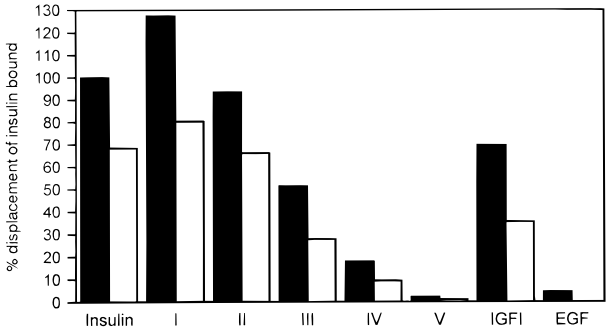

FIGURE 6: Displacement of insulin bound to intact spheroplasts by insulin analogues. Spheroplasts from cells, which had been cultured in succinate medium (see Experimental Procedures), were incubated in succinate (filled bars) or glucose (open bars) medium for 60 min at 30 °C. Thereafter, identical numbers of spheroplasts were incubated with 10 μCi of [^{125}I]monoiodo[A_{14}]insulin in the absence or presence of 10 μM competing hormone for 60 min at 4 °C and then centrifuged through a cushion of Ficoll/sucrose. The spheroplast pellets were rapidly rinsed twice with ice-cold 20 mM Hepes/KOH (pH 7.4) plus 1.1 M sorbitol, and subsequently solubilized with 0.5 N NaOH and counted for radioactivity. The difference in radioactivity recovered in the absence and presence of competing hormone was calculated as the percentage of insulin displaced by human insulin in succinate-incubated spheroplasts (set at 100%). Each value represents the mean of four separate incubations using two different spheroplast preparations. The SD values were in the range of 7−12% of the means.

incubation temperature for reduction of internalization and degradation of bound insulin (see Figures 4 and 5) and with 10 μM final concentration of competitor, which enabled discrimination between the various insulin analogues for binding to the partially purified insulin-binding protein (see Figure 2). The number of binding sites was apparently reduced in glucose-induced vs succinate-incubated spheroplasts by 30−40%. The relative potencies of the insulin analogues and growth factors with regard to displacing iodinated insulin from the spheroplasts were identical for cells incubated in glucose and succinate medium, with analogues I and II being roughly as efficient as human insulin in contrast to analogue V and EGF being completely inactive. Importantly, the relative ranking of the insulin analogues with respect to their affinity was the same for binding to intact spheroplasts (Figure 6) and the partially purified insulin-binding protein (see Figure 2 and Table 1). This strongly suggests that the 53-kDa insulin-binding protein is responsible for the specific binding of human insulin to the cell surface of yeast spheroplasts.

DISCUSSION

We identified an insulin-binding protein in yeast by sequential lectin and insulin affinity chromatographies commonly used for purification of the mammalian insulin receptor and provide evidence that it is involved in mediating specific effects of human insulin on enzymes of glycogen and glucose metabolism and the corresponding key regulatory components (i.e., SNF1 kinase). The protein binds human insulin with a K_d of 0.5 μM, can be specifically affinity-cross-linked to iodinated insulin, and consists of a single polypeptide chain with an apparent molecular mass of 53 kDa on both reducing and nonreducing SDS−PAGE indicating monomeric structure. Intact yeast spheroplasts are able to specifically bind and internalize iodinated insulin in a time- and temperature-dependent fashion. The uptake and subsequent degradation of the internalized insulin requires ATP and thus presumably occurs via the endocytotic machinery.

Despite the absence of an endocrine pancreas, material closely resembling vertebrate-type insulin is present in a range of prokaryotes (*E. coli*, *Halobacteria*; see ref *26*) and

in eukaryotic unicellular organisms, such as ciliated protozoa (*Tetrahymena pyriformis*) as well as fungi (*Aspergillus fumigati and Neurospora crassa*), that were grown in simple synthetic media (27). Net production of insulin was demonstrated by an increase in insulin in the cells and the medium during the early logarithmic growth phase of the cells (28). The concept that hormones can be produced by unicellular organisms is substantiated by the finding that these organisms contain materials that resemble other vertebrate-type hormones, such as ACTH, somatostatin, and relaxin (for a review, see ref *29*). The characterization of these materials that resemble vertebrate-type peptide hormones has included specific radioimmunoassays, radioreceptor assays, and bioassays following purification of extracts using size exclusion, ion exchange, and HPLC (*30*).

In subcellular fractions of the yeast *Saccharomyces cerevisiae*, we identified material that cross-reacted with an anti-insulin antibody raised against total porcine insulin in rabbits (E. Gross and W. Bandlow, unpublished observations). This material migrated slightly faster in SDS−PAGE (corresponding to an apparent molecular mass of 4.7−5.0 kDa) than the authentic oxidized porcine peptide hormone (5.5 kDa). The cross-reacting material was found enriched in the microsomes plus plasma membranes (P45 fraction) and in the periplasmic space (supernatant obtained after removal of Zymolyase-treated cells), whereas cytoplasm (S150 fraction), mitochondria (P13 fraction), and nuclei (P5 fraction) were devoid of this material. Cross-reacting material was recognized also by an antibody raised against a carboxy-terminal hexapeptide of the human insulin B-chain. This material was found enriched in RP-18 eluates of periplasmic fractions from Zymolyase-treated cells (apparent molecular mass about 6 kDa).

However, in the few cases where the primary structure of insulin-like material from evertebrates has been elucidated, it became apparent of being highly divergent and displaying striking differences concerning both the length and the sequence of the polypeptide chain from that of the highly conserved (prepro)insulin from vertebrates (31). A pseudogene possessing an insulin-like protein sequence has been cloned from *Neurospora crassa* (G. Muthukumar and J. Lenard, unpublished observations). In contrast, the yeast genome sequence databases do not contain open reading frames that are reminiscent of insulin peptides as yet. However, so far open reading frames coding for >100 amino acids have been considered as potential genes, only, unless they have been identified previously as genes by genetic means. Mammalian preproinsulin, in general, consists of about 100 amino acids (see, e.g., ref *31*). Thus, a gene potentially coding for an insulin-related peptide has to await future identification.

ACKNOWLEDGMENT

We thank Dr. J. Ertl for providing the insulin analogues and Mrs. A. Unkelbach for expert assistance in preparing the figures (all Hoechst Marion Roussel Deutschland GmbH, Frankfurt, Germany).

REFERENCES

1. Müller, G., Welte, S., and Rouveyre, N. (1997) *Diabetologia 40*, A146 (abstract).
2. Myers, M. G., and White, M. F. (1995) *Trends Endocrinol. Metab. 6*, 209−215.
3. Quon, M. J., Butte, A. J., and Taylor, S. I. (1994) *Trends Endocrinol. Metab. 5*, 369−376.
4. White, F. M., and Kahn, C. R. (1994) *J. Biol. Chem. 269*, 1−4.
5. Müller, G., and Bandlow, W. (1989) *Biochemistry 28*, 9957−9967.
6. Müller, G., and Bandlow, W. (1993) *J. Cell Biol. 122*, 325−336.
7. Müller, G., Groβ, E., Wied, S., and Bandlow, W. (1996) *Mol. Cell. Biol. 16*, 442−456.
8. Müller, G., Schubert, K., Fiedler, F., and Bandlow, W. (1992) *J. Biol. Chem. 267*, 25337−25346.
9. Müller, G., and Zimmermann, R. (1987) *EMBO J. 6*, 2099−2107.
10. Popov, N., Schmitt, M., Schulzeck, S., and Matthies, H. (1975) *Acta Biol. Med. Ger. 34*, 1441−1446.
11. Wessel, D., and Flügge, U. I. (1984) *Anal. Biochem. 138*, 141−143.
12. Lee, J., and Pilch, P. F. (1994) *Am. J. Physiol. 266*, C319−C334.
13. Rosen, O. M. (1989) *Diabetes 38*, 1508−1511.
14. Hofmann, K., Romovacek, H., Titus, G., Ridge, K., Raffensperger, J. A., and Finn, F. M. (1987) *Biochemistry 26*, 7384−7390.
15. Jacobs, S., Hazum, E., Schechter, Y., and Cuatrecasas, P. (1979*) Proc. Natl. Acad. Sci. U.S.A. 261*, 4918−4921.
16. Yip, C. C., Yeung, C. W. T., and Moule, M. L. (1978) *J. Biol. Chem. 253*, 1723−1745.
17. Trischitta, V., Wong, K.-Y., Brunetti, A., Scalisi, R., Vigneri, R., and Goldfine, I. D. (1989) *J. Biol. Chem. 264*, 5041−5046.
18. Krupp, M., and Lane, D. M. (1981) *J. Biol. Chem. 256*, 1689−1694.
19. Kahn, C. R., and Baird, K. (1978) *J. Biol. Chem. 253*, 4900−4906.
20. Kosmakos, F. C., and Roth, J. (1980) *J. Biol. Chem. 255*, 9860−9869.
21. Klein, H. H., Freidenberg, G. R., Matthaei, S., and Olefsky, J. M. (1987) *J. Biol. Chem. 262*, 10557−10564.
22. Eckel, J., and Reinauer, H. (1988) *Biochem. J. 249*, 111−116.
23. Kublaoui, B., Lee, J., and Pilch, P. F. (1995) *J. Biol. Chem. 270*, 59−65.
24. Bevan, A. P., Krook, A., Tikerpae, J., Seabright, P. J., Siddle, K., and Smith, G. D. (1997) *J. Biol. Chem. 272*, 26833−26840.
25. Bergeron, J. J. M., Cruz, J., Khan, M. N., and Posner, B. I. (1985) *Annu. Rev. Physiol. 47*, 383−403.
26. LeRoith, D., Shiloach, J., Roth, J., and Lesniak, M. A. (1981) *J. Biol. Chem. 256*, 6533−6536.
27. Le Roith, D., Shiloach, J., Roth, J., and Lesniak, M. A. (1980) *Proc. Natl. Acad. Sci. U.S.A. 77*, 6184−6188.
28. LeRoith, D., Shiloach, J., Heffron, R., Rubinovitz, C., Tanenbaum, R., and Roth, J. (1985) *Can. J. Biochem. Cell Biol. 63*, 839−849.
29. Blundell, T. L., and Humbel, R. E. (1980) *Nature 287*, 781−787.
30. LeRoith, D., Delahunty, G., Wilson, G. L., Roberts, C. T., Shemer, J., Hart, C., Lesniak, M. A., Shiloach, J., and Roth, J. (1985) *Recent Progr. Horm. Res. 42*, 549−587.
31. Sures, I., Goeddel, D. V., Gray, A., and Ullrich, A. (1980) *Science 208*, 57−59.
32. Munson, P. J., and Rodbard, D. (1980) *Anal. Biochem. 107*, 220−239.

BI972072H